www.czasopisma.pan.pl PAN POLSKA AKADEMIA NAUK www.journals.pan.pl

A R C H I V E S O F M E T A L L U R G Y A N D M A T E R I A L S

Volume 58 2013 Issue 1

DOI: 10.2478/v10172-012-0159-4

B. HADAŁA*, Z. MALINOWSKI*, T. TELEJKO*, A. CEBO-RUDNICKA*, A. SZAJDING*

INFLUENCE OF THE FINITE ELEMENT MODEL ON THE INVERSE DETERMINATION OF THE HEAT TRANSFER COEFFICIENT DISTRIBUTION OVER THE HOT PLATE COOLED BY THE LAMINAR WATER JETS

WPŁYW MODELU METODY ELEMENTÓW SKOŃCZONYCH NA WSPÓŁCZYNNIKA WYMIANY CIEPŁA WYZNACZANY Z ROZWIĄZANIA ODWROTNEGO PROCESU LAMINARNEGO CHŁODZENIA PŁYTY METALOWEJ

The industrial hot rolling mills are equipped with systems for controlled cooling of hot steel products. In the case of strip rolling mills the main cooling system is situated at run-out table to ensure the required strip temperature before coiling. One of the most important system is laminar jets cooling. In this system water is falling down on the upper strip surface. The proper cooling rate affects the final mechanical properties of steel which strongly dependent on microstructure evolution processes. Numerical simulations can be used to determine the water flux which should be applied in order to control strip temperature. The heat transfer boundary condition in case of laminar jets cooling is defined by the heat transfer coefficient, cooling water temperature and strip surface temperature. Due to the complex nature of the cooling process the existing heat transfer models are not accurate enough. The heat transfer coefficient cannot be measured directly and the boundary inverse heat conduction problem should be formulated in order to determine the heat transfer coefficient as a function of cooling parameters and strip surface temperature. In inverse algorithm various heat conduction models and boundary condition models can be implemented. In the present study two three dimensional finite element models based on linear and non-linear shape functions have been tested in the inverse algorithm. Further, two heat transfer boundary condition models have been employed in order to determine the heat transfer coefficient distribution at the hot plate cooled by laminar jets. In the first model heat transfer coefficient distribution over the cooled surface has been approximated by the witch of Agnesi type function with the expansion in time of the approximation parameters. In the second model heat transfer coefficient distribution over the cooled plate surface has been approximated by the surface elements serendipity family with parabolic shape functions. The heat transfer coefficient values at surface element nodes have been expanded in time by the cubic-spline functions. The numerical tests have shown that in the case of heat conduction model based on linear shape functions inverse solution differs significantly from the searched boundary condition. The dedicated finite element heat conduction model based on non-linear shape functions has been developed to ensure inverse determination of heat transfer coefficient distribution over the cooled surface in the time of cooling. The heat transfer coefficient model based on surface elements serendipity family is not limited to a particular form of the heat flux distribution. The solution has been achieved for measured temperatures of the steel plate cooled by 9 laminar jets.

Keywords: head transfer coefficient, finite element model, inverse solution

Nowoczesne linie walcowania blach na gorąco posiadają instalacje do wymuszonego chłodzenia. Jego celem jest kontrolowanie szybkości zmian temperatury blachy w całej objętości zapewniając tym wymaganą strukturę i własności mechaniczne. Chłodzenie jest prowadzone w końcowej części linii technologicznej, w której nad górną i pod dolną powierzchnią gorącego pasma umieszczone są urządzenia dostarczające wodę chłodzącą. Z uwagi na sposób podawania wody chłodzącej można je podzielić na trzy główne systemy: chłodzenie laminarne, chłodzenie z użyciem kurtyn wodnych oraz chłodzenie natryskiem wodnym. W istniejących liniach walcowniczych można spotkać kombinacje poszczególnych systemów. Projektowanie systemów chłodniczych jest trudne i musi być wspomagane przez modele matematyczne i numeryczne wymiany ciepła między gorącą powierzchnią blachy a wodą i otoczeniem. Podstawowe znaczenie dla symulacji procesu ma przyjęcie poprawnych wartości współczynników wymiany ciepła, których znajomość w dużej mierze determinuje dokładność obliczeń. Współczynnik wymiany ciepła nie może być zmierzony bezpośrednio i konieczne jest zastosowanie rozwiązańodwrotnych zagadnienia przewodzenia ciepła. W algorytmach odwrotnych możliwe jest użycie różnych modeli do rozwiązania równania przewodzenia ciepła. Zastosowane modele w istotnym stopniu wpływają na jakość rozwiązania odwrotnego. W pracy przedstawiono wyniki testów dwóch modeli przewodzenia ciepła opartych na liniowych i nieliniowych funkcjach kształtu w algorytmie metody elementów skończonych. Testowano również dwa modele aproksymacji warunku brzegowego. Wybrany model warunku brzegowego i model metody elementów skończonych wykorzystujący nieliniowe funkcje kształtu zastosowano do wyznaczenia współczynnika wymiany ciepła w procesie chłodzenia gorącej płyty stalowej 9 strumieniami wody swobodnie opadającej na jej powierzchnię.

* AGH UNIVERSITY OF SCIENCE AND TECHNOLOGY, DEPARTMENT OF HEAT ENGINEERING AND ENVIRONMENT PROTECTION, 30-059 KRAKÓW, AL. MICKIEWICZA 30, POLAND

Uzyskano rozwiązanie przedstawiające rozkład współczynnika wymiany ciepła i gęstości strumienia ciepła na powierzchni płyty w czasie jej chodzenia.

1. Introduction

During the hot rolling operations the strip losses heat mainly by radiation and convection to surrounding air and cooling water. In the roll gap the strip also losses heat to the rolls, but the time of contact is very short (milliseconds) and the total heat losses are relatively small. However, the strip surface temperature drop can be high to about 600°C. More dramatic changes of the strip surface temperature are observed during descaling with high pressure water jets where the strip surface temperature falls to about 100°C. At the end of hot rolling line the strip temperature is in the range of 800-1000°C and the strip must be cooled down to the required coiling temperature [1]. During water cooling the strip undergoes rapid changes of temperature which have significant effect on material structure and properties. Thus, the strip temperature control in the hot rolling operations is very important and involves computer modeling. The most important is a proper determination of heat transfer boundary conditions during water cooling at run-out table before coiling. There are several methods of cooling one of them are laminar flow cylindrical water jets or water curtains placed above the strip. Hatta et al. [2, 3] have developed empirical equations for heat transfer coefficient (HTC) while cooling 18Cr-8Ni steel plate 10 mm thick with water curtain. Two equations have been proposed, one for nucleate and transition boiling when water is in direct contact with the plate surface (wetting zone). The second equations have been proposed for film boiling. The heat transfer coefficient for wetting zone has been approximated by the local Nusselt number for laminar flow of water over the plate surface. The heat transfer boundary condition model has been verified based on the plate temperature measurements by 3 thermocouples attached to the bottom plate surface (not cooled by water). The assumption of the laminar flow of water and model validation by temperature measurements 10 mm below the water cooled surface are the primary drawbacks in the heat transfer model. The inverse solution for heat transfer coefficient determination while cooling AISI 304L steel by one axially symmetrical water jet have been presented by Wang et al. [4]. The plate thickens was 25 mm and the plate temperature was measured by 4 thermocouples located 2.5 mm below the cooled surface. The solution has been obtained on the basis of axially symmetrical heat conduction model. Similar inverse solution for one spray nozzle was proposed by Malinowski at al. [5]. Inverse solutions based on axially symmetrical models are limited to one spray or jet nozzle only. Inverse solution based on three dimensional heat conduction model are required for heat transfer coefficient determination for plate cooling by a set of water jets, water sprays or water curtains. This class of solutions have been presented by Kim et al. [6] and Zhou et al. [7] but only for the simulated temperature sensor indications. The solutions have been obtained for a large number of simulated sensors, at least one sensor is required in element or at element node in the plane of simulated sensors locations. Such a large number of sensors will change material structure and its properties in case of physical experiment. In the paper the inverse solution based on three dimensional heat conduction model for measured plate temperatures has been obtained.

2. Plate cooling model

The temperature field in the plate cooled by laminar water jets has been determined from the transient heat conduction equation:

$$\frac{\partial T}{\partial \tau} = \frac{\lambda}{\rho c}\left(\frac{\partial^2 T}{\partial x_1^2} + \frac{\partial^2 T}{\partial x_2^2} + \frac{\partial^2 T}{\partial x_3^2}\right) + q_v \tag{1}$$

where: c – specific heat, T – temperature, q_v – internal heat source, x, y, z – rectangular coordinates, τ – time, λ – thermal conductivity, ρ – density.

The solution of equation (1) gives the plate temperature field for the specified boundary conditions at the plate surfaces. At the water cooled upper plate surface convection boundary condition has been specified:

$$\dot{q}\,(x_1 = h, x_2, x_3, \tau) = \alpha\,(x_1 = h, x_2, x_3, \tau)\,(T_s - T_a) \tag{2}$$

where: h – plate height, T_s – plate surface temperature, T_p – water temperature.

Heat transfer coefficient α at the water cooled surface has been defined as a function of surface coordinates and the time of cooling. Two boundary condition models have been tested in the inverse solution to the heat conduction problem (IHCP).

In the first boundary condition model (Model A) for the approximation of the HTC distribution over the cooled surface the witch of Agnesi type function has been chosen:

$$\alpha(x_1 = h, x_2, x_3, \tau) = \frac{[\alpha_{max}(\tau)]^3}{(c\,(\tau)\,(x_2 - b/2))^2 + [\alpha_{max}(\tau)]^2} \tag{3}$$

where: b determines width of the plate, $c(\tau)$ is a time dependent parameter and $\alpha_{max}(\tau)$ is the maximum value of the heat transfer coefficient at $x_2 = b/2$. Cubic-spline functions have been chosen for the expansion in time of the parameters $c(\tau)$ and $\alpha_{max}(\tau)$:

$$c\,(\tau) = \sum_{i=1}^{4} H_i(\eta) p_i \tag{4}$$

$$\alpha_{max}\,(\tau) = \sum_{j=1}^{4} H_j(\eta) p_j \qquad \text{for } \eta \in (0, 1) \tag{5}$$

Accuracy of the HTC distribution in the time of cooling can be improved dividing the cooling time into periods for which $\tau \in (\tau_1, \tau_2)$. In this case the local coordinate η is given by:

$$\eta = \frac{\tau - \tau_1}{\tau_2 - \tau_1} \tag{6}$$

The cubic-spline functions H_j have the following form:

$$\begin{aligned} H_1 &= 1 - 3\eta^2 + 2\eta^3 \\ H_2 &= 3\eta^2 - 2\eta^3 \\ H_3 &= \eta - 2\eta^2 + \eta^3 \\ H_4 &= -\eta^2 + \eta^3 \end{aligned} \tag{7}$$

The parameters p_j define the values of c and α_{max} parameters and their derivatives with respect to time at nodes of approximation.

The boundary condition model A is limited to the HTC distributions for which maximum value of HTC takes place at the water jets line for $x_2 = b/2$. However, HTC strongly depends on the cooled surface temperature and the model A might not be able correctly reflect HTC distribution for boiling heat transfer. More general model B has been developed for which the HTC distribution over the cooled surface has been approximated by surface elements with quadratic shape functions serendipity family:

$$\alpha(x_1 = h, x_2, x_3, \tau) = \sum_{i=1}^{8} N_i P_i(\tau) \tag{8}$$

where N_i are quadratic shape functions serendipity family:

$$\begin{gathered} N_1 = (1-\xi_1)(1-\xi_2)(-\xi_1-\xi_2-1)/4 \\ N_2 = \left(1-\xi_1^2\right)(1-\xi_2)/2 \\ N_3 = (1+\xi_1)(1+\xi_2)(\xi_1-\xi_2-1)/4 \\ N_4 = \left(1-\xi_2^2\right)(1+\xi_1)/2 \\ N_5 = (1+\xi_1)(1+\xi_2)(\xi_1+\xi_2-1)/4 \\ N_6 = \left(1-\xi_1^2\right)(1+\xi_2)/2 \\ N_7 = (1-\xi_1)(1+\xi_2)(-\xi_1+\xi_2-1)/4 \\ N_8 = \left(1-\xi_2^2\right)(1-\xi_1)/2 \text{ for } \xi_1 \in (-1,+1) \text{ and } \xi_2 \in (-1,+1) \end{gathered} \tag{9}$$

where ξ_1, ξ_2 are natural coordinates of the surface element. In the case of boundary condition model B the cooled surface is divided into rectangular elements. For each element equation (8) has been used to approximate the HTC distribution. Functions $P_i(\tau)$ describe the heat transfer coefficient variation at nodes of elements in the time of cooling. At each element node the function$P_i(\tau)$ has the following form:

$$P_i(\tau) = \sum_{j=1}^{3} W_j(\eta) p_{ij} \tag{10}$$

where the parabolic-spline functions W_j are given by:

$$\begin{gathered} W_1 = 1 - 3\eta + 2\eta^2 \\ W_2 = 4\eta - 4\eta^2 \\ W_3 = 2\eta^2 - \eta \quad \text{for} \quad 0 \leqslant \eta \leqslant 1. \end{gathered} \tag{11}$$

In the case of the boundary condition model B the set of unknown parameters p_{ij} which have to be determined in the inverse heat conduction model is composed of the heat transfer coefficient values at nodes of approximation.

At the lower plate surface, which is free from water, radiation boundary condition has been specified:

$$\dot{q}(x_1 = 0, x_2, x_3, \tau) = 5,67 \cdot 10^{-8} \frac{T_s^4 - T_k^4}{\frac{1}{\varepsilon_s} + \frac{S_s}{S_k}\left(\frac{1}{\varepsilon_k} - 1\right)} \tag{12}$$

where: S_k – cooling chamber surface, S_s – plate surface,T_k – cooling chamber surface temperature, ε_s – emissivity of the plate surface, ε_k – emissivity of the cooling chamber surface. The heat flux at the lower plate surface which is not cooled by water is very small (about 0.5%) compared to heat flux for water cooling and natural convection neglected in equation (12) and possible inaccuracy in emissivity determination will not have any practical influence on the inverse solution to the HTC at the water cooled surface.

In the IHCP solution only part of the plate is considered as shown in Fig. 1. At the side surfaces of the plate which cover less than 13% of the total boundary surface zero heat flux boundary conditions have been assumed:

$$\dot{q}(x_1, x_2 = 0, x_3, \tau) = -\lambda \frac{\partial T}{\partial x_2} = 0 \tag{13}$$

$$\dot{q}(x_1, x_2 = b, x_3, \tau) = -\lambda \frac{\partial T}{\partial x_2} = 0 \tag{14}$$

$$\dot{q}(x_1, x_2, x_3 = 0, \tau) = -\lambda \frac{\partial T}{\partial x_3} = 0 \tag{15}$$

$$\dot{q}(x_1, x_2, x_3 = l, \tau) = -\lambda \frac{\partial T}{\partial x_3} = 0 \tag{16}$$

where: b – width of the plate, l – length of the plate.

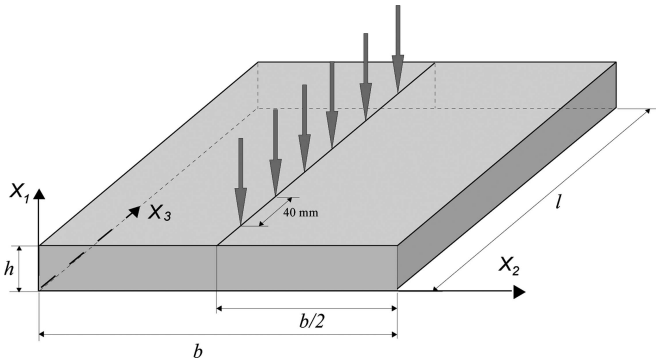

Fig. 1. The plate cooling model employed in the inverse solution to the 3D heat conduction problem

It is expected that the heat gains at the side surfaces of the plate neglected in the IHCP will be less than 0.05% of the heat flux for water cooling.

In the heat conduction equation (1) q_v represents the internal heat source. In the case of steel plate cooling heat generation due to phase transformation should be included in the IHCP. However, it would require a separate model for heat generation dedicated for the inverse solution. In the present study inconel alloy and steel grade which do not involve phase transformation in the examined temperature range has been selected to avoid influence of heat generation on the HTC determination. In such cases q_v =0.

The unknown parameters p_j or p_{ij} which define the HTC distribution in developed boundary conduction models A and B have to be determined by minimizing the objective function:

$$E(p_i) = \sum_{m=1}^{Nt} \sum_{n=1}^{Np} \left(Te_n^m - T_n^m\right)^2 \tag{17}$$

where: p_i is the vector of the unknown parameters composed of parameters p_j or p_{ij}, Nt – number of the temperature sensors, Np – number of the temperature measurements performed by one sensor in the time of cooling, Te_n^m – the plate temperature measured by the sensor m at the time τ_n, T_n^m –

the plate temperature at the location of the sensor m at the time τ_n calculated from the finite element solution to the heat conduction equation (1).

To solve the heat conduction equation (1) finite element method has been used. By employing the weighted residuals method to Eq. (1) two finite element models have been developed. In the first model linear shape function has been used. In the second model non linear weighting and shape functions have been employed. The detailed description of the two finite element models has been presented in [8, 9].

3. Inverse solutions to simulated temperature sensor indications

The developed model for the inverse determination of heat transfer coefficient has been first tested based on simulated temperature sensor indications. The simulations have been performed for the inconel alloy with the conductivity and specific heat presented in Fig. 2. The inconel density has been assumed as 8470 kg/m^3. Simulations have been performed for the plate with the dimensions of h =10 mm, b =100 mm and l =200 mm. It has been assumed that the initial plate temperature is T_o =700°C. The simulated temperature sensors indications have been achieved in direct simulations of the plate cooling. The temperature variations have been simulated at 12 points located 1 mm below the cooled surface at x_1 =9 mm. Locations of points in $x_2 - x_3$ plane have been presented in Fig. 3. In the simulated plate cooling the boundary condition at the upper plate surface has been described by Eq. (3) with the parameter α_{max} = 1000 W/(m^2·K) and c = 50000. At the other boundary surfaces heat loses has been neglected. The assumed parameters describe constant in time heat transfer coefficient distribution over the cooled surface with the thermal symmetry at the plane $x_2 = b/2$. Since there is no change of the HTC in x_3 direction the temperature variation at point P_1 is the same as at points: P_4, P_5, P_8, P_9, P_{12}. At point P_2 temperature varies in time in the same way as at points: P_3, P_6, P_7, P_{10}, P_{11}. Simulated temperature sensor indications obtained in the direct solution have been presented in Fig. 4. Two numerical tests S1 and S2 have been performed based on simulated temperature sensor indications. Finite element models based on linear (Simulation S1) and non linear (Simulation S2) form functions have been tested in the inverse solution to the heat conduction problem.

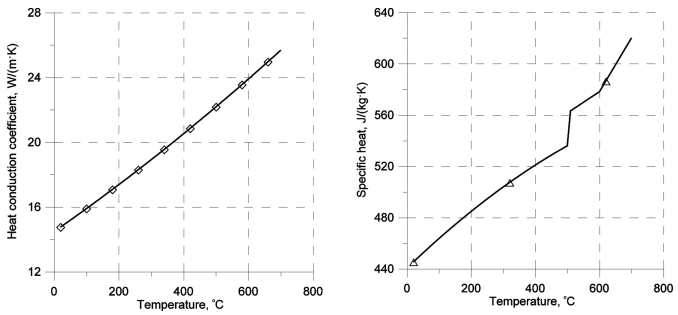

Fig. 2. Heat conduction coefficient and specific heat as functions of temperature for the inconel alloy

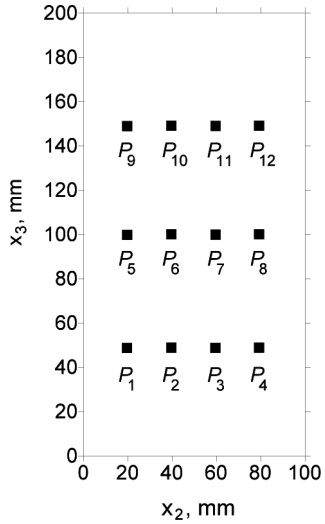

Fig. 3. Locations of the simulated temperature sensors in the $x_2 - x_3$ plane 1 mm below the cooled surface

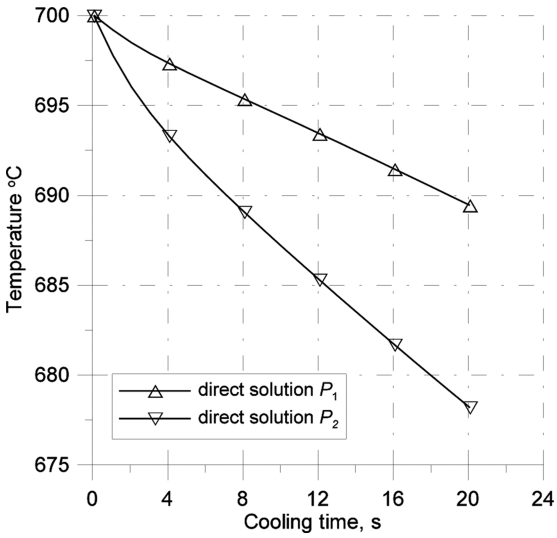

Fig. 4. Simulated temperature sensor indications at point P_1 and P_2 for the modeled boundary condition described by equation (3) with α_{max} = 1000 W/(m^2·K) and c = 50000

- Simulation S1 – linear weighting and shape functions have been employed in the finite element solution to the heat conduction equation (1). The plate has been divided into 11×10×2 isoperimetric elements as shown in Fig. 5. The solution to the heat conduction problem depends on 396 degrees of freedom, which are temperatures at elements nodes.
- Simulation S2 – non linear weighting and shape functions have been employed in the finite element solution to the heat conduction equation (1). The plate has been divided into 2×2×1 prism elements in x_1, x_2 and x_3 direction, respectively. The solution to the heat conduction problem depends on 144 degrees of freedom composed of temperatures and temperature derivatives at prism elements nodes.

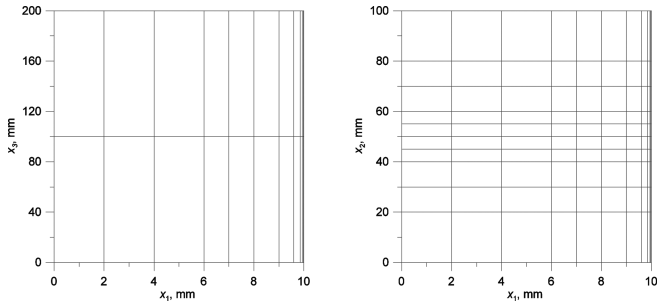

Fig. 5. Division of the cooled plate into linear elements employed in the simulation S1

In the inverse solutions S1 and S2 the boundary condition defined by Eq. (3) with the parameter α_{max} = 1000 W/(m^2·K) and c = 50000 have been searched for in the approximate form given by Eq. 8. The cooled surface has been divided into 3 serendipity elements as shown in Fig. 6. The heat transfer coefficient distribution presented in Fig. 7b has been approximated by quadratic shape functions (9). Changes of the HTC values at elements nodes have been extended in time of cooling in the same way as parameter c in Eq. (4) with the cubic – spline functions (7). The approximation of the boundary condition shown in Fig. 7b with the use of 3 serendipity elements involves 72 degrees of freedom to be determined by minimizing the objective function (17). Minimizations of the objective function (17) have converged to the average difference between computed temperatures and the simulated temperature sensors indications at the level of 0,186 K and 0,06 K for the S1 and S2 case (Table 1), respectively. The level of the error norm indicates that the solution S2 based on non linear finite element model should give better approximation of the prescribed boundary condition. In Fig. 8 and Fig. 9 the HTC variations at the thermal symmetry plane for $x_2 = b/2$ have been compared. Solution S1 (Fig. 8) overestimates the HTC at the symmetry plane from 40% to 80%. In the case of solution S2 the highest error do not exceeds 20%. In Fig. 7 HTC distributions on the cooled surface have been compared.

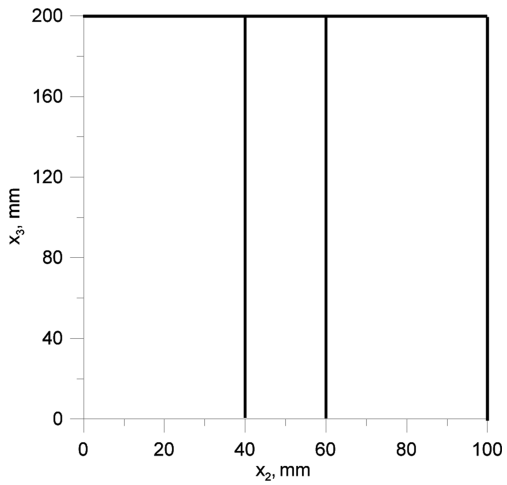

Fig. 6. Division of the cooled surface into serendipity family elements employed for the heat transfer coefficient approximation

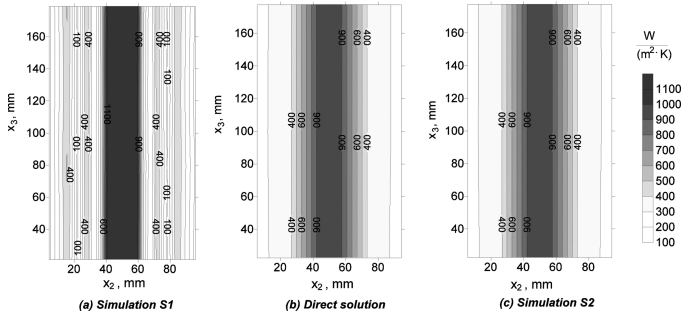

Fig. 7. Comparison of the prescribed boundary condition (b) with the inverse solutions based on the linear finite element model (a) and the non linear finite element model (c)

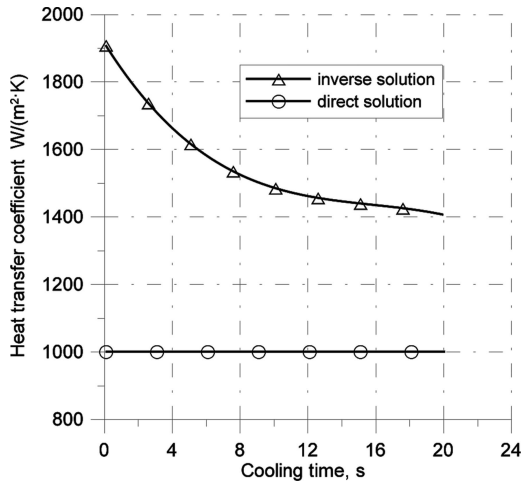

Fig. 8. Comparison of the modeled HTC at the symmetry plane at $x_2 = b/2$ with the inverse solution S1 based on linear finite element model

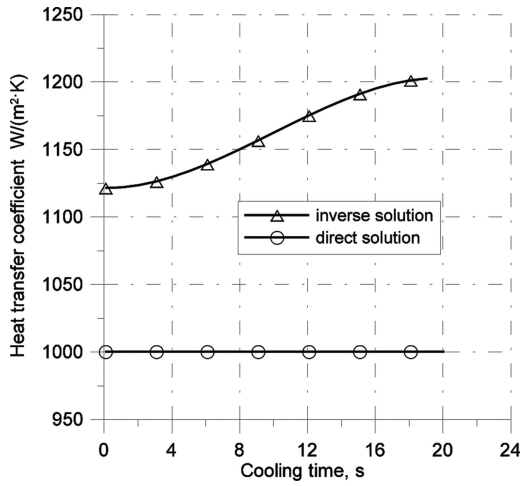

Fig. 9. Comparison of the modeled HTC at the symmetry plane at $x_2 = b/2$ with the inverse solution S2 based on non linear finite element model

The inverse solution S2 based on non linear finite element model has given results very close to the modeled boundary condition presented in Fig. 7b. The same conclusions can be drawn out to the heat flux distributions presented in Fig. 10. The solution S1 based on linear shape functions gives heat flux distribution over the cooled surface (Fig. 10a) which differs

essentially from the modeled case shown in Fig. 10b. The plate surface temperature after 20 s of cooling has been shown in Fig. 11. The average temperature error presented in Table 1 is low for both simulations S1 and S2. However, as it can be seen in Fig. 11 good agreement between modeled temperature field (Fig. 11b) and the inverse solution based on linear finite element model has been obtained only at locations of simulated measurement points. Inverse solution based on non linear shape functions has given temperature field (Fig. 11c) very similar to the modeled case (Fig. 11b). The conducted numerical test have shown that the inverse solution based on non linear form functions can be employed in determining heat transfer boundary conditions at the cooled plate with good accuracy.

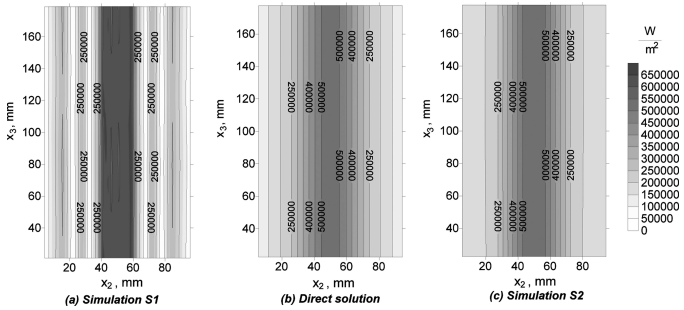

Fig. 10. Comparison of the prescribed heat flux (b) with the inverse solutions based on the linear finite element model (a) and the non linear finite element model (c)

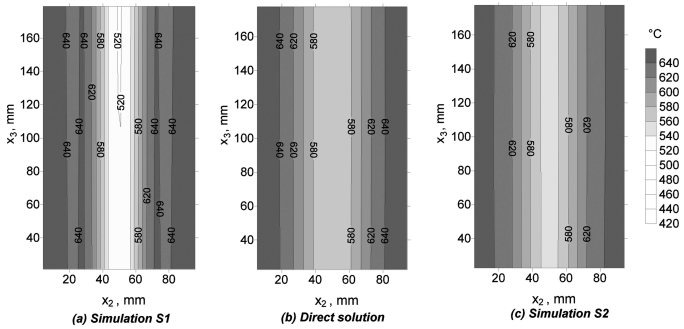

Fig. 11. Comparison of the cooled surface temperature obtained in the direct simulation (b) with the inverse solutions based on the linear finite element model (a) and the non linear finite element model (c)

TABLE 1

Average differences between computed temperatures and the simulated temperature sensors indications

Maximum value of HTC, W/(m^2· K)	Heat condition model	Average error, K
1000	S1	0,186
	S3	0,06

4. Inverse solution to measured temperatures while water jets cooling

The developed inverse method based on non linear shape functions has been employed to determine the heat transfer coefficient while cooling steel plate with 9 water jets. Steel plate 210 mm in width, 300 mm in length and 8 mm in height has been heated in the electric furnace to the uniform temperature of 811°C. Hot plate has been pulled from the furnace and cooled by 9 water jets placed in lines at the middle of the plate (Fig. 12.). Water jets have been situated 0,39 m above the plate. Water flux was 39,04 dm^3/(s·m^2) and water temperature was 16,9°C. The plate temperature have been measured by 20 thermocouples located 2 mm below the cooled surface. Thermocouples have been situated in 5 rows. Distance between thermocouples in a row was 20 mm and the distance between rows was 50 mm. The test sample has been made from H13JS steel. The heat conductivity (Fig. 13), specific heat (Fig. 13) and density (Fig. 14) as functions of temperature for H13JS steel have been determined from the data published in [10]. The cooled surface has been divided into 4 serendipity elements in x_3 direction and 2 elements in x_2 direction. Thus, the distribution of the HTC coefficient defined by Eq. (8) has been approximated by 8 surface elements. The HTC approximation in time at each node of the surface elements has been achieved dividing the time of cooling into 6 periods. The model of the HTC approximation over the cooled surface and in the time of cooling requires 481 p_{ij} parameters in Eq. 10. The parameters have been determined by minimizing the error norm (17). The inverse solution converged to the average error of 3.01 K between measured and computed temperatures. In Fig. 15 temperatures measured by one row of thermocouples situated at the middle of the plate length have been compared with the computed temperatures. The computed temperatures compare very well to the measured data over the time of cooling. The inverse solution has given complete information about the heat transfer coefficient and heat flux variations over the cooled surface as functions of time. In Fig. 16 the HTC distribution over the cooled surface after 20 s

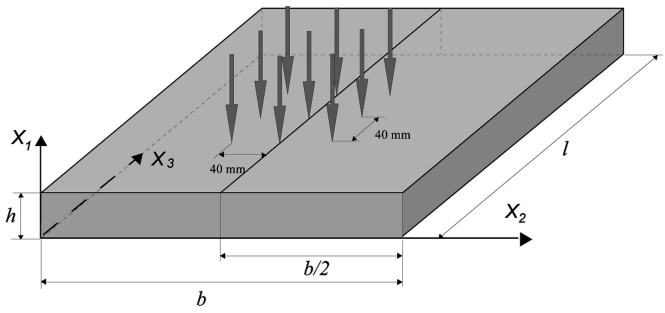

Fig. 12. Schematic for the plate cooling by 9 water jets employed in the 3D inverse solution to the measured data

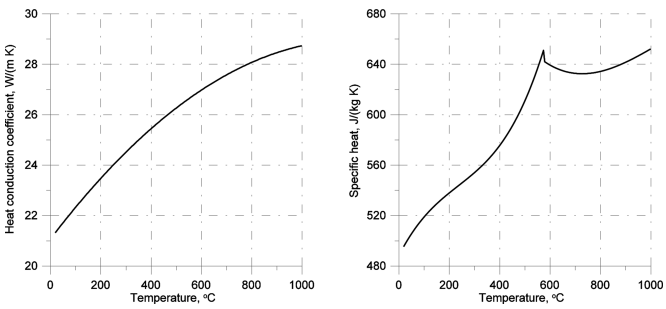

Fig. 13. Heat conduction coefficient and specific heat as functions of temperature for H13JS steel

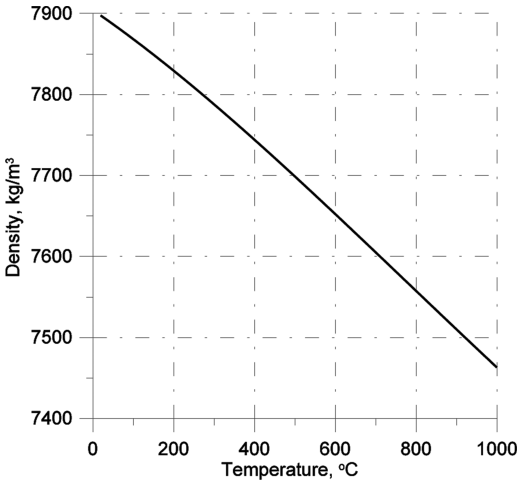

Fig. 14. Density as function of temperature for H13JS steel

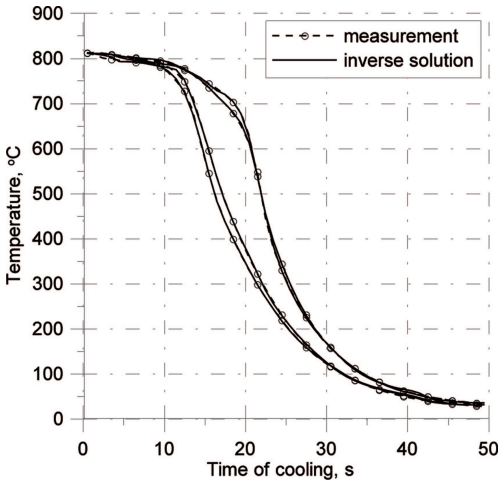

Fig. 15. Comparison of the measured and computed temperatures for the thermocouples located at the middle of the plate length 2 mm below the cooled surface

of cooling has been presented. The HTC varies significantly from 100 W/(m^2· K) to 12000 W/(m^2· K) over the cooled surface. It affects the cooled surface temperature as it has been shown in Fig. 17. The plate temperature below the water jets has dropped to about 50°C but at the distance of 40 mm from the water jets the plate temperature at the same time is still very height and reaches 750°C. Presented HTC and temperature distributions over the cooled surface have shown that the plate cooling with the water jets results in significant non uniformity of the heat transfer boundary conditions. Numerical modeling of such processes will encounter serious problems with the boundary condition determination. For practical implementations average values can be used. In Fig. 18 average heat transfer coefficient as function of average surface temperature determined based on obtained inverse solution has been presented. The average heat transfer coefficient has been calculated from the average heat flux (Fig. 19) over the square of 80×80 mm below the water jets. Presented in Fig. 18 and Fig. 19 average heat transfer coefficient and average heat flux as functions of the average surface temperature can be calculated from the equations:

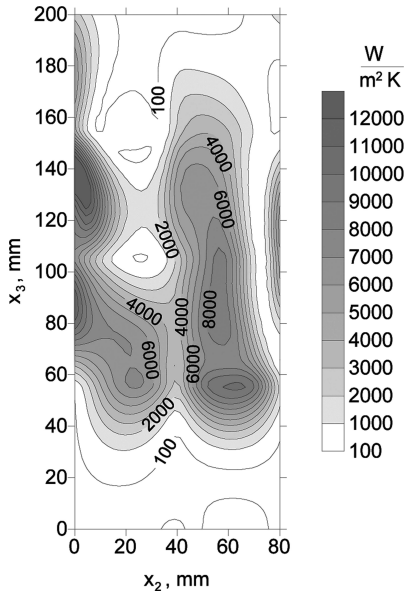

Fig. 16. Heat transfer coefficient distribution over the plate surface after 20 s of water jets cooling for H13JS steel and water flux 39,04 dm^3/(s·m^2)

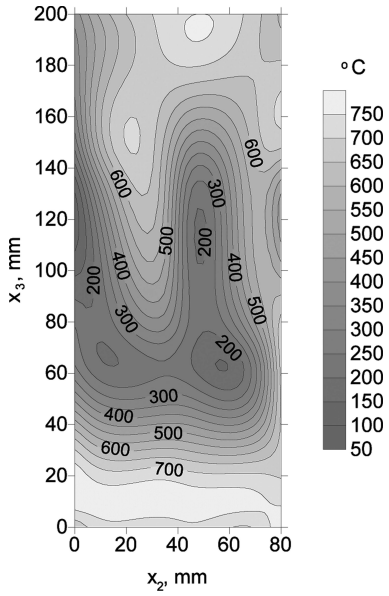

Fig. 17. Temperature distribution at the plate surface after 20 s of water jets cooling for H13JS steel and water flux 39,04 dm^3/(s·m^2)

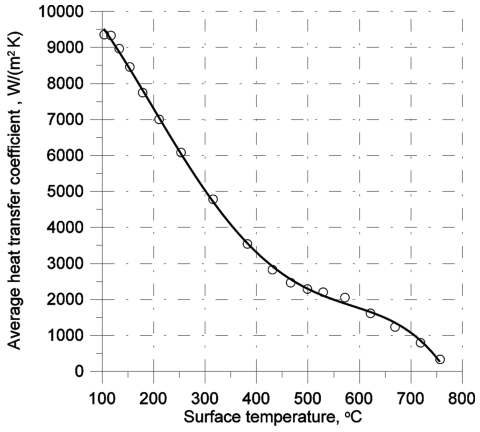

Fig. 18. Average heat transfer coefficient variation versus average plate surface temperature for H13JS steel and water flux 39,04 dm^3/(s·m^2)

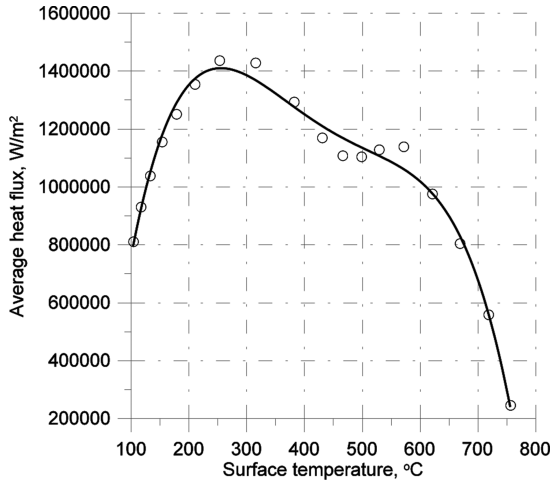

Fig. 19. Average heat flux variation versus average plate surface temperature for H13JS steel and water flux 39,04 $dm^3/(s{\cdot}m^2)$

$$\alpha_{avg} = 10917,89 - 4,640322283t_{avg} - 0,1112395936t_{avg}^2 + 2,527505886{\cdot}10^{-4}t_{avg}^3 - 1,615307042{\cdot}10^{-7}t_{avg}^4 \quad (18)$$

$$\dot{q}_{avg} = -1000294,7 + 25838,87325t_{avg}97,16632886t_{avg}^2 + 0,1507293345t_{avg}^3 - 8,53505648{\cdot}10^{-5}t_{avg}^4 \quad (19)$$

where: α_{avg} – average heat transfer coefficient, $W/(m^2{\cdot}K)$; $\dot{q}_{avg}$– average heat flux, $W/(m^2)$; t_{avg} – average plate surface temperature, °C.

Equations (18) and (19) are valid for the temperature range from 100°C to 750°C and water flux about 39 $dm^3/(s{\cdot}\ m^2)$.

5. Conclusions

Three dimensional inverse solution to the boundary heat conduction problem has been developed. The inverse model is based on finite element solution to the heat conduction in the plate cooled by water jets. Two direct models have been tested in the inverse algorithm. Numerical tests performed for simulated temperature sensor indications have shown that implementation of the finite element model based on linear shape functions leads to good agreement between computed and measured data only at temperature sensor locations. It makes very difficult to achieve reliable heat flux distributions at the cooled surface. The problem has been solved developing dedicated three dimensional model based on non linear cubic–spline functions. Implementation of higher order shape functions has allowed to limit the number of thermocouples to 20 for the plate cooled by 9 water jets. The heat flux distribution at steel plate surface cooled from 811°C to the room temperature by water jets has been obtained. Based on heat flux distribution over the plate surface in the time of cooling variation of the average heat transfer coefficient as a function of average plate surface temperature has been achieved. The developed formulas defining average heat flux and average heat transfer coefficient can be implemented in numerical simulations of steel strip cooling at run out table in hot rolling plants.

Acknowledgements

The work has been financed by the Ministry of Science and Higher Education of Poland, Grant No NR15 0020 10.

REFERENCES

[1] G. Béranger, G. Henry, G. Sanz, The book of steel, Intercept Ltd, New York (1996).
[2] N. Hatta, Y. Tanaka, H. Takuda, J. Kokado, A numerical study on cooling process of hot steel plates by water curtain, ISIJ International **29**, 673-679 (1989).
[3] N. Hatta, H. Osakabe, Numerical modeling for cooling process of a moving hot plate by a laminar water curtain, ISIJ International **29**, 919-925 (1989).
[4] H. Wang, W. Yu, Q. Cai, Experimental study of heat transfer coefficient on hot steel plate during water jet impingement cooling, Journal of Materials Processing Technology **219**, 1825-1831 (2012).
[5] Z. Malinowski, T. Telejko, B. Hadała, A. Cebo-Rudnicka, Implementation of the axially symmetrical and three dimensional finite element models to the determination of the heat transfer coefficient distribution on the hot plate surface cooled by the water spray nozzle, Key Engineering Materials **504-506**, 1055-1060 (2012).
[6] S.K. Kim, J.-S. Lee, W.I. Lee, A solution method for a nonlinear three-dimensional inverse heat conduction problem using the sequential gradient method combined with cubic-spline function specification, Numerical Heat Transfer, Part B **43**, 43-61 (2003).
[7] J. Zhou, Y. Zhang, J.K. Chen, Z.C. Feng, Inverse estimation of surface heating condition in a three-dimensional object using conjugate gradient method, International Journal of Heat and Mass Transfer **53**, 2643-2654 (2010).
[8] A. Gołdasz, Z. Malinowski, B. Hadała, Study of heat balance in the rolling process of bars, Archives of Metallurgy and Materials **54**, 3, 685-694 (2009).
[9] Z. Malinowski, T. Telejko, B. Hadała, A. Cebo-Rudnicka, 3D FEM Model for the Inverse Determination of the Heat Flux Distribution on the Hot Plate Surface Cooled by Water, Proceedings of Numerical Heat Transfer 2012 International Conference, eds. A.J. Nowak, R. A. Białecki, Wrocław, Poland, 82-91 (2012).
[10] A. Goldsmith, T.E. Waterman, H.J. Hirschhorn, Handbook of thermophysical properties of solid materials **2**, Pergamon Press, New York (1962).

Received: 10 April 2012.